FUNCTIONS OF CYTOPLASMIC FIBERS IN INTRACELLULAR MOVEMENTS IN BHK-21 CELLS

EUGENIA WANG and ROBERT D. GOLDMAN

From the Department of Biology, Case Western Reserve University, Cleveland, Ohio 44106, and the Department of Biological Sciences, Carnegie-Mellon University, Pittsburgh, Pennsylvania 15213. Dr. Wang's present address is The Rockefeller University, New York 10021

ABSTRACT

After trypsinization and replating, BHK-21 cells spread and change shape from a rounded to a fibroblastic form. Time-lapse movies of spreading cells reveal that organelles are redistributed by saltatory movements from a juxtanuclear position into the expanding regions of cytoplasm. Bidirectional saltations are seen along the long axes of fully spread cells. As the spreading process progresses, the pattern of saltatory movements changes and the average speed of saltations increases from 1.7 μm/s during the early stages of spreading to 2.3 μm/s in fully spread cells. Correlative electron microscope studies indicate that the patterns of saltatory movements that lead to the redistribution of organelles during spreading are closely related to changes in the degree of assembly, organization, and distribution of microtubules and 10-nm filaments.

Colchicine (10 μg/ml of culture medium) reversibly disassembles the microtubule-10-nm filament complexes which form during cell spreading. This treatment results in the disappearance of microtubules and the appearance of a juxtanuclear accumulation of 10-nm filaments. These changes closely parallel an inhibition of saltatory movements. Within 30 min after the addition of the colchicine, pseudopod-like extensions form rapidly at the cell periphery, and adjacent organelles are seen to stream into them. The pseudopods contain extensive arrays of actinlike microfilament bundles which bind skeletal-muscle heavy meromyosin (HMM). Therefore, in the presence of colchicine, intracellular movements are altered from a normal saltatory pattern into a pattern reminiscent of the type of cytoplasmic streaming seen in amoeboid organisms. The streaming may reflect either the activity or the contractility of submembranous microfilament bundles. Streaming activity is not seen in cells containing well-organized microtubule-10-nm filament complexes.

KEY WORDS saltatory movements · cytoplasmic streaming · microfilaments · 10-nm filaments · microtubules

The major type of non-Brownian intracellular organelle movement seen in cultured cells is termed saltatory movement. This type of movement has been extensively described by Rebhun (33, 34, 36, 37) as "discontinuous stop-go periods of motions, interspersed by periods of rest, i.e., particles may suddenly move many microns in seconds." The movements are generally linear and bidirectional (36, 37, 49). The velocity of saltatory movement varies from 1 to 30 μm/s,

J. CELL BIOLOGY © The Rockefeller University Press 0021-9525/78/1201-0708$1.00
Volume 79 December 1978 708-726

with the highest frequency of saltations in the 2–4 μm/s range (37). Although Freed and Lebowitz (9) have set 4 μm as the smallest particle excursion considered to be a saltation, many workers have accepted ~1 μm as the limit (37). Very little is known about the generation of motive force for such movements, nor is it known how the force is regulated or transmitted to particles to produce motion. Three types of cytoplasmic fibers – microtubules, 10-nm filaments, and microfilaments – have all been implicated as the possible force-generating fibrous structures in various aspects of cell motility (see for example, references 8, 14, 19, 21, 27, 32, and 42). It is therefore of considerable importance to examine the phenomenology of intracellular movements and to decipher the possible involvement of cellular fibrous structures in these movements. The present study provides an analysis of changes in saltatory movements and organelle distribution during the spreading and shape-formation processes of BHK-21 cells. Both organelle saltations and organelle distributions can be closely related to the presence, localization, and organization of microtubules and 10-nm filaments.

This study has also revealed that there is an inhibition of saltatory movement and an induction of cytoplasmic streaming after addition of colchicine to spreading BHK-21 cells. Similar observations have also been made on oocytes and HeLa cells (4, 35). This streaming activity resembles that seen in amoeboid cells. In the present investigation, submembranous, actinlike microfilament bundles are found in areas of streaming activity. However, no microtubules or 10-nm filaments have been found in these areas. These results are discussed in terms of the possible contractile activity of microfilament bunldes for streaming in cytoplasmic regions which are devoid of microtubules and 10-nm filaments.

MATERIALS AND METHODS

Cell Cultures

Cultures of baby hamster kidney cells (BHK-21/C13) (47) were grown at 37°C in BHK-21 medium (Grand Island Biological Co., Grand Island, N. Y.) supplemented with 10% calf serum, 10% tryptose phosphate broth, 100 U/ml penicillin, and 100 μg/ml streptomycin. Subconfluent cultures were used in all experiments.

Light Microscopy

The procedure for the preparation of the coverslip cultures has been described elsewhere (10, 11). Cells were observed with a Zeiss photomicroscope II (Carl Zeiss, Inc., N. Y.) equipped with phase-contrast and polarized-light optics. Intracellular movements were recorded on either 35-mm Plus-X film with a still camera or 16-mm Plus-X film with a Sage time-lapse cinematography system (Sage Instruments Div., Orion Research Inc., Philadelphia, Pa.). Cell cultures were maintained at 37°C with a Sage air stream incubator. A Dvorak-Stotler culture chamber (Nicholson Precision Instruments, Inc., Bethesda, Md.) was used for taking 16-mm movies so that fresh culture medium could be introduced without disturbing the microscope field.

Time-Lapse Cinematographic Analysis

The pattern of organelle movements was recorded at a rate of 120 frames per minute, or two frames per second. To measure movements, the films were projected on a graphic screen with a stop-motion projector (Photo-optical Data Analyzer, L & W Projector, Van Nuys, Calif.).

Saltatory path lengths (SPL) were determined by measuring the distance of individual saltations on the movie screen. The actual SPL was calculated by dividing these measurements by the total magnification factor. The duration of individual saltations was determined by dividing the number of movie frames over which the movement occurred by 2. For example, a certain saltation occupied eight frames of the movie film and therefore spanned a period of 4 s. The speed of organelle movement was determined by dividing the distance moved by the time taken by the movement.

Statistical Analysis of Particle Movement

To determine whether or not the motility of organelles observed in the early stages of spreading differed significantly from that observed in the later stages, Student's *t* test was applied to the data. For this purpose, SPL and the speeds of 106 particles were determined in 10 different cells at stage 2 of spreading, and also of 80 particles for 10 different cells at stage 4 of spreading. Standard deviations were also used to compare measurements of movements in cells at different stages of spreading.

Electron Microscopy

Cells were fixed in Petri dishes for 30 min at room temperature in 1% glutaraldehyde in phosphate buffered saline (PBS) (0.05 M KH_2PO_4-NaOH buffer, pH 7.2, containing 0.01 M sucrose, 0.03 M $MgCl_2$, and 0.003 M $CaCl_2$). After two to three brief rinses with PBS, the cells were postfixed for 30 min in 1% OsO_4 in PBS. Cells were then rinsed twice with PBS, dehydrated rapidly through increasing concentrations of ethanol, and flat-embedded in Epon 812 (26).

The Epon-embedded cells which were of interest were selected using a Leitz inverted microscope (E. Leitz, Inc., Rockleigh, N. J.) and marked with a needle controlled by a Leitz micromanipulator. These cells were cut from the main block of plastic with a punch mounted in a drill press. The resulting blocks were remounted for

thin-sectioning parallel to the plane of cell-substrate contact. Sections were cut with a diamond knife on a Sorvall Porter-Blum MT-2 microtome (DuPont Instruments-Sorvall, DuPont Co., Wilmington, Del.) and were mounted on Formvar-carbon coated copper grids. The sections were stained with hot uranyl acetate (25) and lead citrate (38). Ultrastructural observations were made with either a JELCO 7-H or Philips 200 electron microscope.

Glycerination and Heavy Meromyosin Binding in Colchicine-Treated Cells

Heavy meromyosin (HMM) was prepared by the methods of Szent-Gyorgi (48) and Pollard and Weihing (31). Cells with streaming activity were obtained by treatment of spreading cultures with colchicine (10 μg/ml) for 1 h. Glycerination and HMM binding were carried out according to the method described by Chang and Goldman (6). The cells were then processed for electron microscopy as described above.

RESULTS

Light- and Electron-Microscope Observations of Organelle Distribution during Cell Spreading

A definite pattern of changes in shape and organelle distribution occurs as cells spread upon a substrate after trypsinization and replating. Several stages of the spreading process can be defined, each characterized by its overall shape, type of organelle movement, and the distribution of organelles. These stages occur at approximately the same time periods after initial plating. If one designates stage 0 (Fig. 1*a*) as the stage at which BHK-21 cells are round in shape in a freshly trypsinized cell suspension, four additional stages can be defined:

STAGE 1: Approx. 30 min after attachment. Most of the cells are still round. Membrane ruffling and pinocytosis are seen at their peripheries and a prominent juxtanuclear clear region is evident (Figs. 1*b* and *c*).

STAGE 2: Approx. 30–60 min after attachment. This stage is characterized by the formation of large sheets of cytoplasm which expand over the substrate (Fig. 1*d*), and are devoid of most organelles, except for a few pinocytotic vacuoles. Most of the organelles aggregate around the relatively clear juxtanuclear region during this stage. When observed with polarized-light optics, this clear region is birefringent (Figs. 2*a* and *b*).

STAGE 3: Approx. 60–120 min after attachment. During this stage, the cells start to assume a fibroblastic shape (Fig. 1*e*). Ruffling activities and pinocytosis are restricted to two or three regions located at the tips of cytoplasmic processes. Organelles begin to move away from their perinuclear positions as the juxtanuclear birefringent region becomes dispersed towards the cell periphery (Figs. 2*c* and *d*).

STAGE 4: 3–4 h after attachment. The cells are well spread on the substrate and have attained the characteristic shape of fibroblasts (Fig. 1*f*). The juxtanuclear birefringent region has disappeared or is very small. Relatively little membrane ruffling or pinocytotic activity is seen. Many organelles have moved into long cytoplasmic extensions (Fig. 1*g*). Filamentous mitochondria are oriented with their long axes parallel to the long axes of these cytoplasmic extensions. When observed with polarized-light optics, a birefringent streak is seen frequently and is usually parallel to the long axis of the cell (Figs. 2*e* and *f*).

To determine the relationship of microtubules, 10-nm filaments, and microfilaments to these changing patterns of organelle movements, the ultrastructure of cells at different stages of spreading has been studied. The birefringent juxtanuclear cap observed during stages 1 and 2 of spreading contains a mass of 10-nm filaments (Fig. 3, and 3*a*). Organelles are distributed randomly in the cytoplasm outside this region (Fig. 3). In general, short segments of microtubules appear randomly scattered in the cytoplasm. The large, clear sheet of cytoplasm seen at stage 2 primarily contains ribosomes, microfilament bundles, and membrane-bound vesicles (Fig. 4, and 4*a*). Very few microtubules and no 10-nm filaments are seen in this region. Observations of cells in stages 3 and 4 indicate that the juxtanuclear mass of 10-nm filaments is smaller, and that many filaments appear to extend out into the cytoplasm from the nuclear region (Fig. 5). Arrays of microtubules and 10-nm filaments are seen oriented parallel to each other along the major cell processes (Fig. 6). Most organelles are distributed in the cytoplasm among parallel arrays of microtubules and 10-nm filaments (Fig. 6, 6*a*, and *b*).

Analysis of Saltatory Movements

Many organelles show classical saltatory behavior: they make sudden jumping movements over relatively long distances through the cytoplasm; the movements are rapid and can last for several

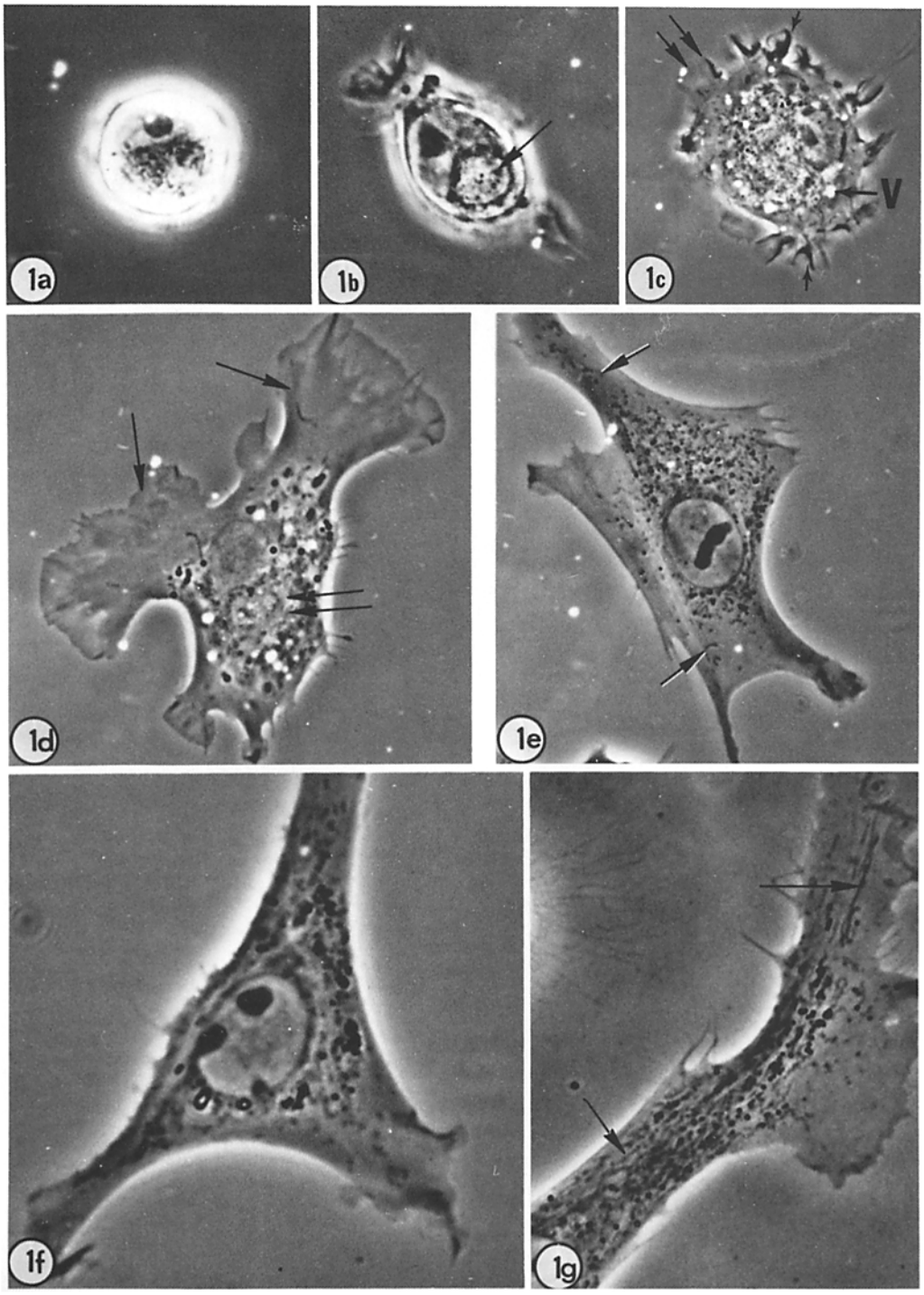

FIGURE 1 Phase-contrast micrographs of cells at various stages of spreading. Fig. 1*a*: An unattached, spherical BHK-21 cell. × 1,620. Fig. 1*b* and *c*: Attached cells observed 30 min after plating. Note the juxtanuclear clear region (arrow shown in Fig. 1*b*). Active membrane ruffling (arrows) and pinocytotic vesicles (*V*) are shown in Fig. 1*c*. × 1,400. Fig. 1*d*: 1 h after plating cells. Note the presence of large clear sheets of cytoplasm (arrows) and the aggregation of organelles in the perinuclear region. Double arrows indicate the juxtanuclear clear region. × 1,350. Fig. 1*e*: 2 h after plating. Note the fibroblastic shape and the distribution of organelles such as mitochondria into the peripheral regions of cytoplasm (arrows). × 1,620. Fig. 1*f*: A cell observed 4 h after plating. × 1,700. Fig. 1*g*: A fibroblastic process that contains longitudinally oriented arrays of filamentous mitochondria (arrows) and other organelles. 4 h after plating. × 1,700.

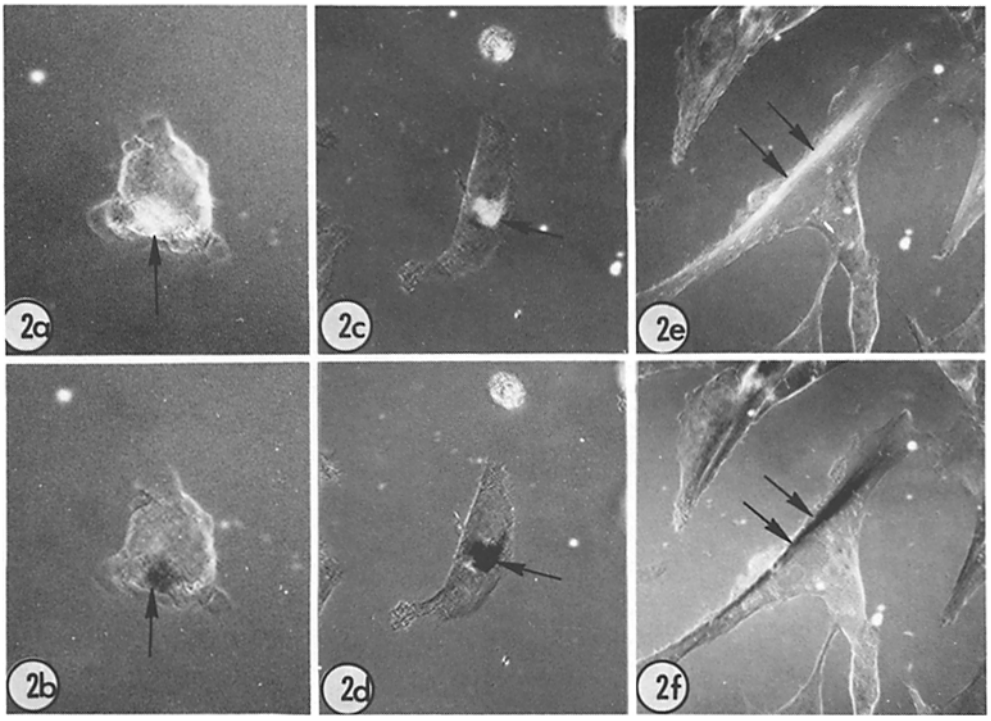

FIGURE 2 A series of polarized-light micrographs of the same living cell at various stages of spreading. These micrographs demonstrate the typical changes in intracellular birefringence which occur during spreading. In each pair, micrographs are shown at opposite compensator settings. Fig. 2*a* and *b*: Note the spherical birefringent region at 1 h after replating (arrows). × 850. Fig. 2*c* and *d*: At 2 h note the "reeling out" of the juxtranuclear birefringent region (arrows). × 525. Fig. 2*e* and *f*: At 4 h, note the presence of a prominent birefringent streak along the long axis of the cell (arrows). × 400.

seconds; motions of individual organelles can occur simultaneously in opposite directions; and, in general, organelle motions occur independently of neighboring organelles, regardless of proximity.

Time-lapse movies reveal that the number of saltatory movements and the pattern of these movements change considerably during the spreading process. Very few saltations are seen in round cells (stage 1). A significant increase in saltatory activity is observed in cells at stage 2. At this time, the majority of moving organelles display bidirectional movements which occur in a radial fashion in the perinuclear region (Fig. 7). During stage 3 of the spreading process, saltatory movements are usually found in cytoplasmic pathways leading to regions adjacent to ruffled membranes (Fig. 8). As the cells progress to stage 4, most saltatory movements take place along the long axes of the cell processes (Figs. 9 and 10). Movements perpendicular to the long axes of major cell processes have not been observed.

To characterize more precisely the behavior of organelles engaged in saltatory movements, the following properties have been determined: (*a*) the average speed of all saltatory movements monitored during all stages of spreading, (*b*) the average path lengths of saltations during specific stages of spreading, and (*c*) the average duration of individual saltations during specific stages of spreading. Saltatory movements of all types of cytoplasmic organelles which are easily visualized at the resolution of light microscopy have been analyzed. However, because of the abundance of mitochondria, pinocytotic vesicles, and various types of lysosomes in BHK-21 cells, most of the measurements result from the analysis of these three types of organelles.

The speed of saltatory movements in cells at all stages of spreading ranged from 0.7 to 4.1 μm/s. Saltatory movements during stage 2 are slower than those seen in stage 4. In addition, longer SPL are seen in stage 4 when compared to stage 2 (Table I). Most SPL range between 2 and 4 μm in stage 2 and between 4 and 8 μm in the later stages

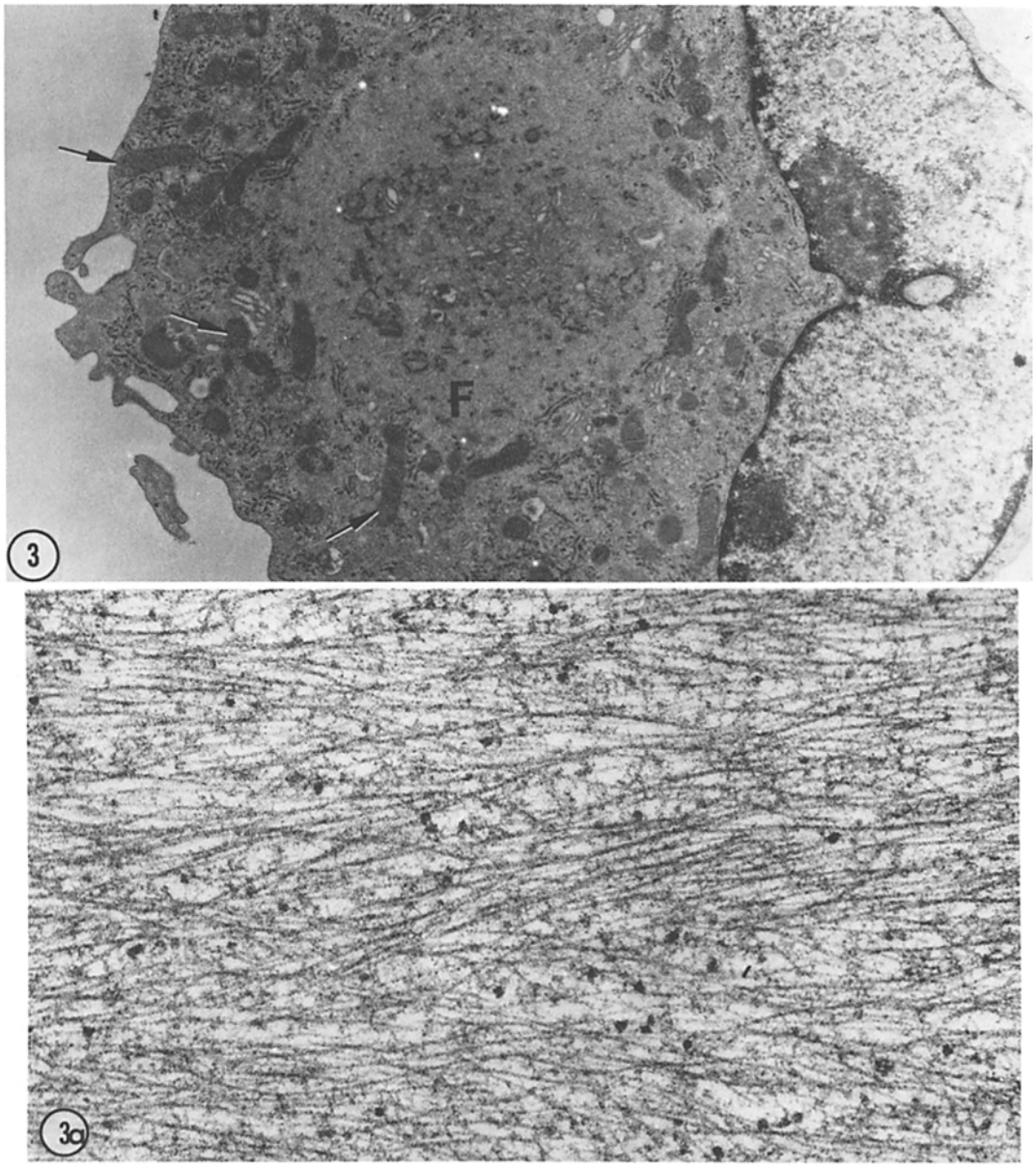

FIGURE 3 Electron micrograph of a cell fixed at the first stage of spreading. Note that the juxtanuclear clear region contains large numbers of 10-nm filaments (*F*), and organelles such as mitochondria surround this region (arrows). × 8,060. Fig. 3*a*: High magnification of a portion of a clear region that shows 10-nm filaments. × 63,200.

of spreading. In addition, the average duration of saltations increases during spreading (see Table I). The value (obtained by applying a Student's *t* test) for the two sets of SPL data for stages 2 and 4 is 10. According to this value, the probability that the two sets of data are similar is <0.001, indicating a significant difference in the motile behavior of organelles between stages 2 and 4.

Intracellular Movements of Colchicine-Treated BHK-21 Cells

Within 30 min after the addition of colchicine

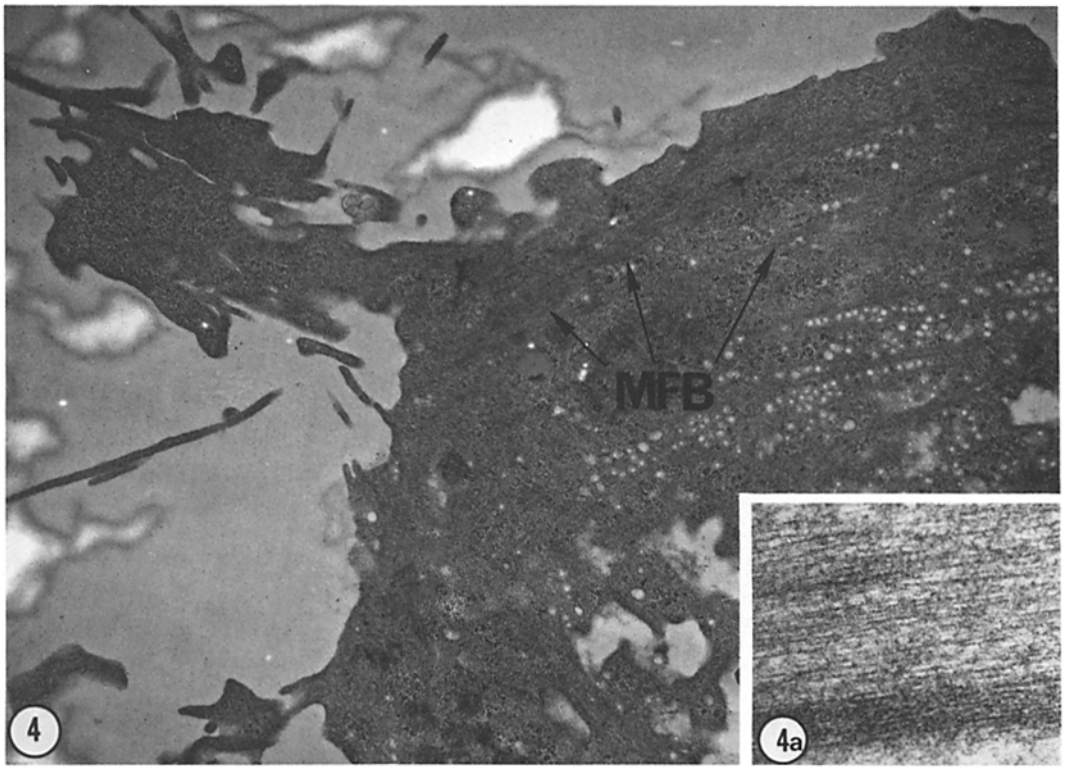

FIGURE 4 Thin section through large clear sheet of cytoplasm shown in Fig. 1*d*. This micrograph demonstrates that this area contains primarily ribosomes, vesicles, and microfilament bundles (MFB). × 5,760. Fig. 4*a*: Higher magnification of the same area showing a portion of an MFB. × 68,000.

(10 μg/ml of culture medium) to cells in stages 2 or 3, saltatory movements cease. Membrane ruffling continues in the presence of colchicine (Fig. 11*a*). Temporary cytoplasmic extensions which resemble pseudopods form, and organelles located in nearby areas stream unidirectionally into these extensions (Fig. 11*b–e*). Organelles, such as mitochondria, appear to be carried in a passive, rolling fashion in the streaming cytoplasm. In any one pseudopod, streaming activity continues for 1–2 min, until the pseudopod becomes filled with cytoplasmic organelles (Fig. 11*e*). Shortly thereafter, the streaming activity ceases and the pseudopod is retracted (Fig. 11*f–i*). During the retraction of the pseudopods, organelles are withdrawn into the main body of the cell. The sequential events of pseudopod formation and cytoplasmic streaming are seen frequently during a 2-h period after the addition of colchicine. Occasionally, a streaming current passes through the nuclear region and causes the nucleus to move in the direction of streaming, often resulting in the nucleus being positioned at the extreme periphery of the cell.

Within 2–3 h after the addition of colchicine, the formation of pseudopods and cytoplasmic streaming are greatly diminished. The fibroblastic shape of BHK-21 cells is altered to a more epithelial-like shape (10). Observations with phase contrast reveal the presence of a region free of organelles adjacent to the nucleus (Fig. 12*a*). Polarized-light observations demonstrate that these juxtanuclear regions are birefringent (Fig. 12*b*).

The effect of colchicine is reversible.When colchicine is removed after 1–2 h of treatment, cytoplasmic streaming ceases and saltatory movements are reinitiated. Within 2–3 h after the effects of colchicine are reversed, the cells regain their fibroblastic shape and the large juxtanuclear birefringent region disappears. Organelles are observed to regain their organized distribution in the cytoplasm (see also reference 10).

Electron microscopy reveals that microtubules

FIGURE 5 Electron micrograph of a cell fixed at the third stage of spreading that demonstrates the extension of 10-nm filaments (*F*) from a juxtanuclear position towards the cell periphery; organelles such as mitochondria are also distributed into peripheral regions of the cytoplasm. × 4,000.

are absent in colchicine-treated cells. 10-nm filaments are seen almost exclusively in the juxtanuclear birefringent region (Fig. 13, and 13*a*). Submembranous bundles of microfilaments are the only fibrous structures distributed normally (Fig. 14, and 14*a*). These are most prominent just beneath the adhesive surface of cells.

Cells with colchicine-induced pseudopods were selected for electron microscopy from flat-embedded preparations on the basis of their resemblance to cells seen in live preparations. These cells were circled out with a micromanipulator by using an inverted microscope, and pseudopod position was noted. The blocks were processed for thin-section-

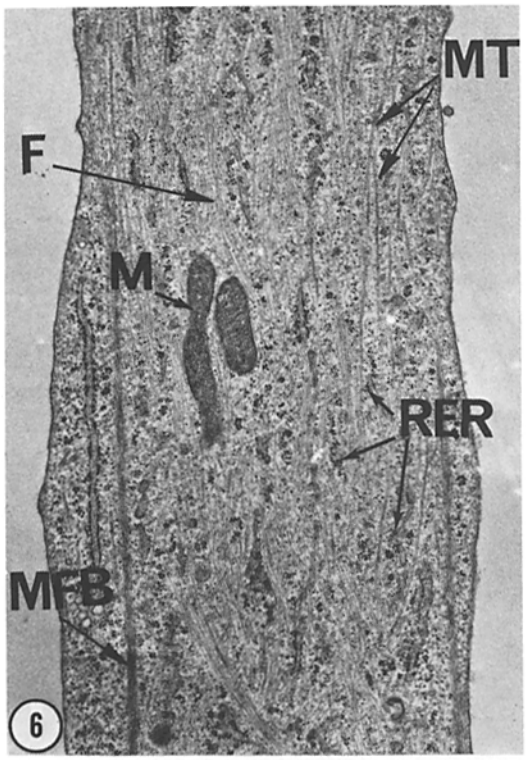

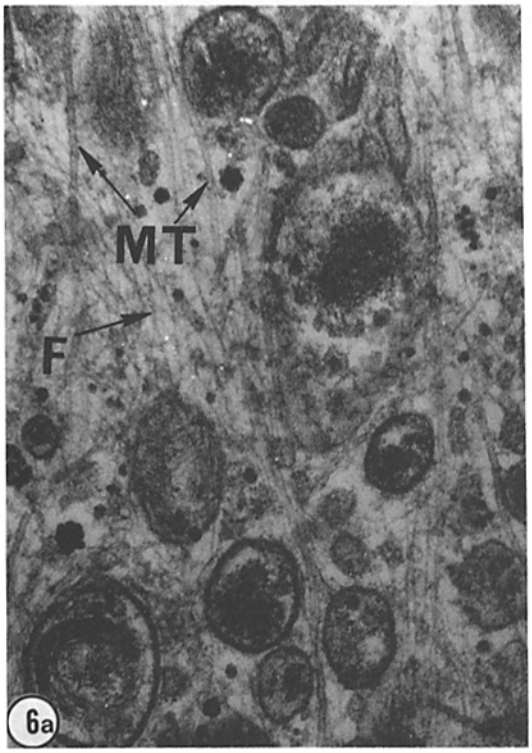

ing so that sections parallel to the plane of cell-substrate contact were obtained. Serial sections were prepared beginning in the region of cell-substrate adhesion and ending at their nonadhesive surfaces. Examination of these sections has demonstrated that microfilament bundles are found in regions of the cortical cytoplasm (adjacent to the substrate) of pseudopods (Fig. 15 and 15*a*). These microfilament bundles are arranged with their long axes oriented along the length of pseudopods, and therefore correspond to the streaming direction. 20 pseudopods have been sectioned and no microtubules nor 10-nm filaments have been found in streaming areas. However, ribosomes, mitochondria, lipid droplets, pinocytotic vesicles, and other organelles have been seen in thin-sections of cytoplasmic areas not adjacent to cell substrate contact (Fig. 16).

Colchicine-treated cells with pseudopods which contain streaming cytoplasm have been glycerinated and treated with rabbit skeletal-muscle HMM. The overall morphology and shape of the pseudopods is preserved throughout the steps involved in glycerination, HMM-treatment, and preparation for electron microscopy (Fig. 17). HMM-decorated microfilament bundles could be found oriented along the length of the pseudopods (Fig. 18). HMM could be removed from microfilaments by treatment with Mg^{++}-pyrophosphate (39). These results demonstrate that the microfilaments found in pseudopods are actinlike in nature.

DISCUSSION

The organization, distribution, and localization of microtubules, 10-nm filaments, and microfilaments are associated with the distribution and movements of organelles in spreading BHK-21 cells. It appears that these fibrous components are the cytoskeletal and contractile structures involved in at least three major types of intracellular move-

FIGURE 6 Electron micrograph taken of a region along the length of a fibroblastic process. Note the parallel arrangement of microtubules (*MT*), 10-nm filaments (*F*). Microfilament bundles (*MFB*) are also present nearer the plasma membrane. Mitochondria (*M*) and rough endoplasmic reticulum (*RER*) are also located along this parallel distribution of cytoplasmic fibers. × 11,080. Fig. 6*a*: Close association of microtubules (*MT*) and 10-nm filaments (*F*) with various types of membrane bound organelles. × 41,660.

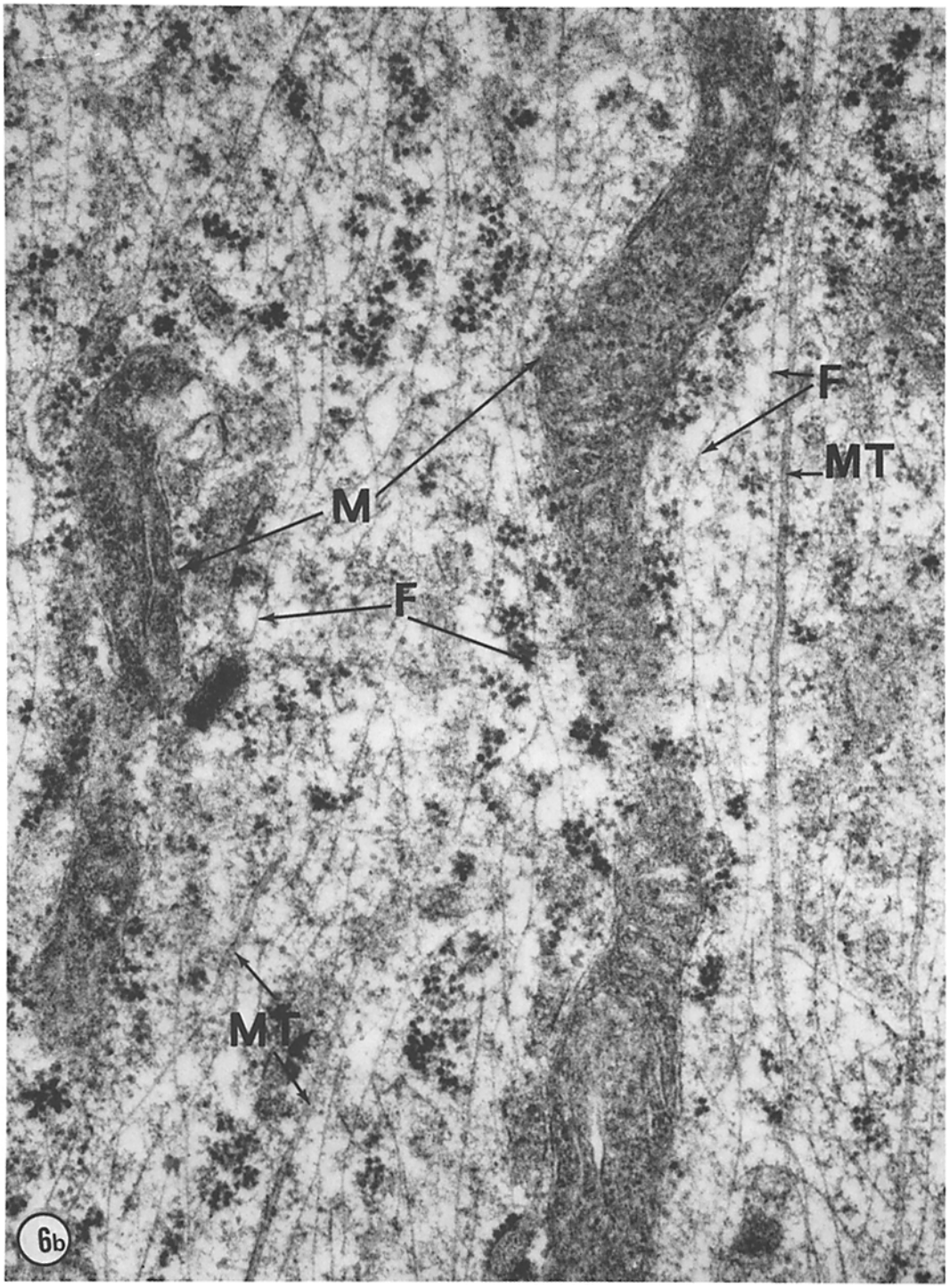

FIGURE 6*b* Higher magnification view showing filamentous mitochondria (*M*), microtubules (*MT*), and 10-nm filaments (*F*). × 53,500.

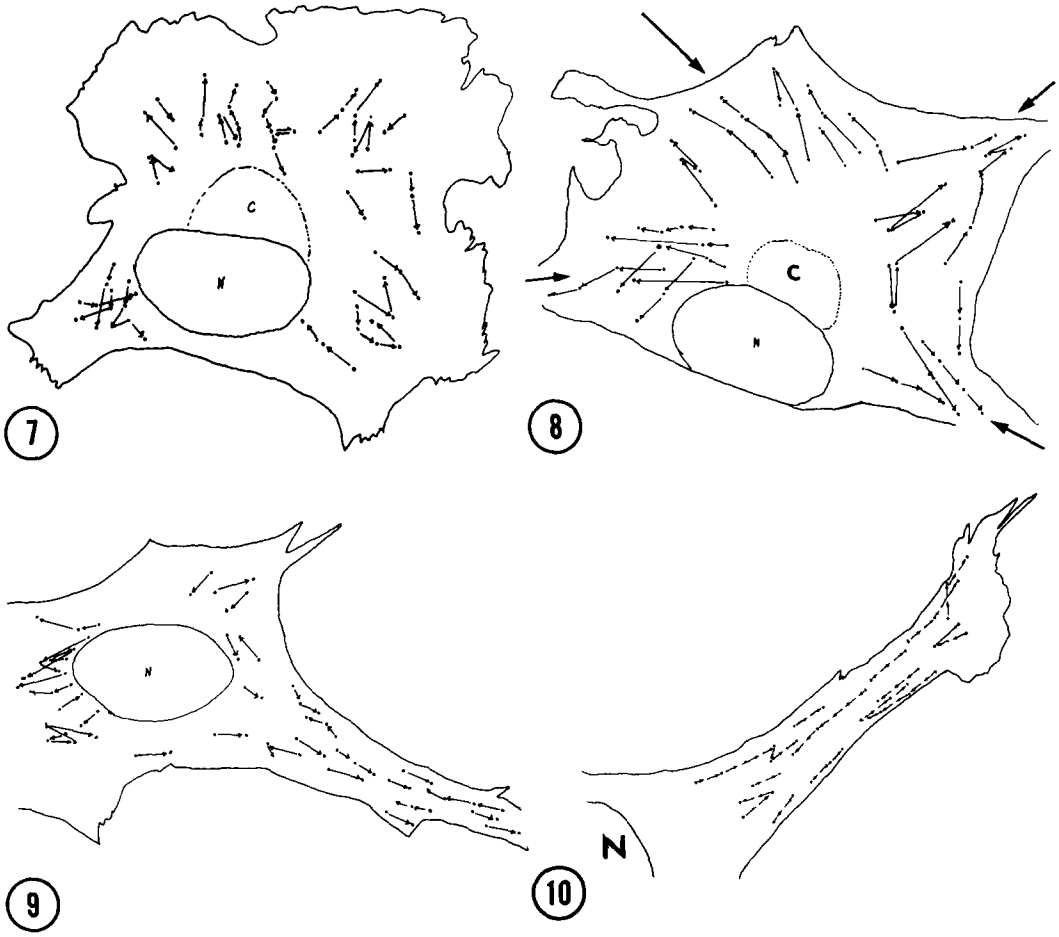

FIGURE 7 A figure that shows the pattern of saltatory pathways in a cell that has progressed to the second stage of the spreading process. Organelles and granules are seen to move in all directions between the nucleus and the cell periphery. This diagram and those seen in Figs. 8–10 are based on time-lapse cinematographic analyses. *C* represents the juxtanuclear clear region.

FIGURE 8 A figure that shows the pattern of saltatory pathways in cells at the third stage of spreading. Note that saltations occur in regions leading toward ruffled membranes (arrows).

FIGURE 9 A figure that demonstrates the pattern of saltatory pathways in a fully spread cell (4 h after initiation of culture). The majority of organelles exhibit bidirectional saltatory movements along the long axis of the cell.

FIGURE 10 A figure that shows the pattern of saltatory pathways in a major fibroblastic process. Most organelles move in directions parallel to the long axis of this process. Movements perpendicular to this long axis have not been seen.

ments: (*a*) organelle distribution from the cell center to the peripheral regions during spreading and shape formation, (*b*) bidirectional saltatory organelle movements, and (*c*) the cytoplasmic streaming which is induced when microtubules-10-nm filament complexes are disrupted with colchicine.

Organelle Distribution

The sequence of events which lead to the distribution of organelles within the cytoplasm corresponds closely to the formation of parallel arrays of microtubules and 10-nm filaments. In freshly trypsinized cells, the majority of microtubules and

TABLE I

Comparison of SPL, Duration, and Speed of Organelle Movements in Cells at Stages 2 and 4 of the Spreading Process

Stage	n*	Average SPL	Range of SPL	Average duration	Average speed
		μm	μm	s	$\mu m/s$
2	106	3.6 ± 1.5‡	1.9–16.7	2.1	1.7
4	80	6.8 ± 2.5‡	2.9–15.5	3.1	2.2

* n = Number of organelles observed.
‡ Standard deviation.

10-nm filaments are concentrated in the perinuclear region, as are most of the organelles. Microfilament bundles are seen in the clear sheets of cytoplasm which form at the cell periphery during the early stages of spreading. However, no larger organelles such as mitochondria or other membrane-bound structures are seen within these areas when they first appear during spreading. Later, organelles migrate into these clear areas coincident with the extension and assembly of microtubules and 10-nm filaments. In fully spread cells, organelles are invariably found in close association with parallel arrays of microtubules and 10-nm

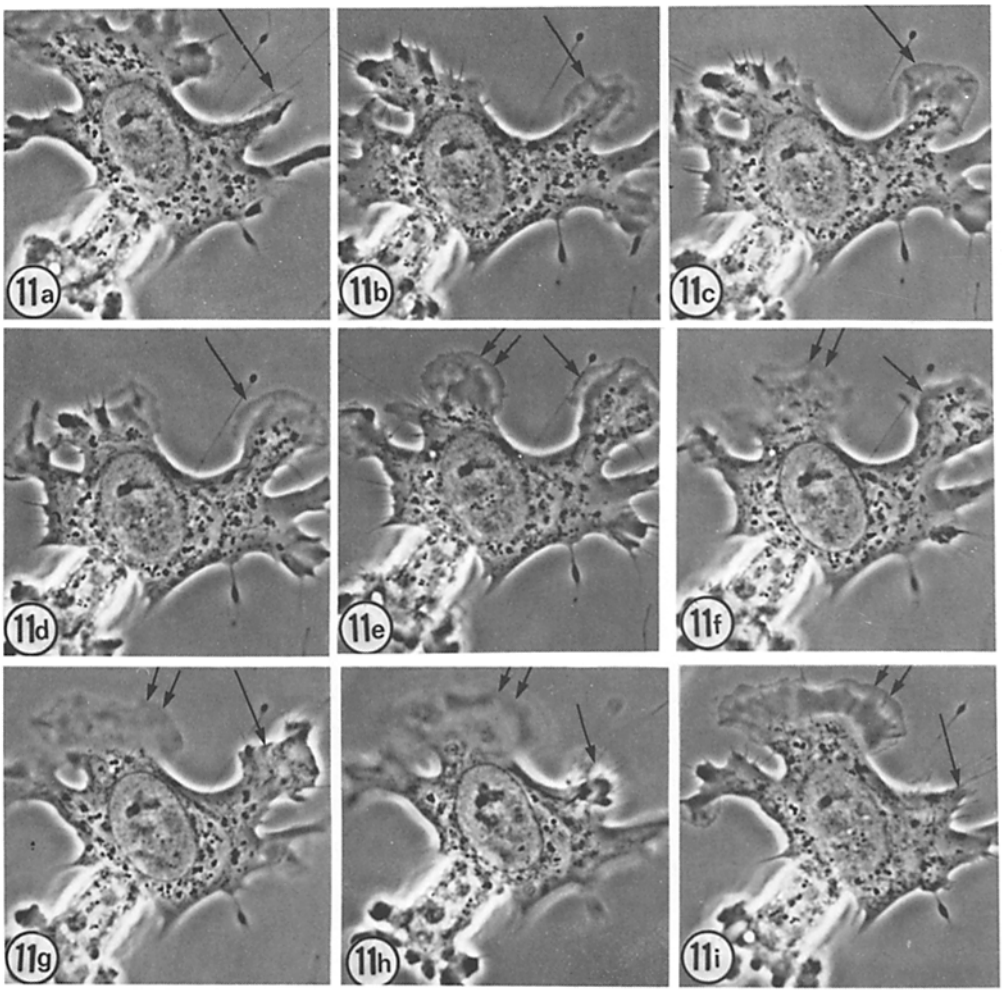

FIGURE 11 A sequence of phase-contrast micrographs that demonstrates the process of pseudopod formation and cytoplasmic streaming in cells that have been treated with 10 μg/ml colchicine for 30 min. × 750. Fig. 11 *a* and *b*: Single arrow points to a forming pseudopod. Fig. 11 *c–e*: Organelles move into the pseudopod (single arrow). Note the formation of another pseudopod (double arrows). Fig. 11 *f*: The pseudopod is filled with organelles. Fig. 11 *g–i*: The pseudopod retracts into the main cell body.

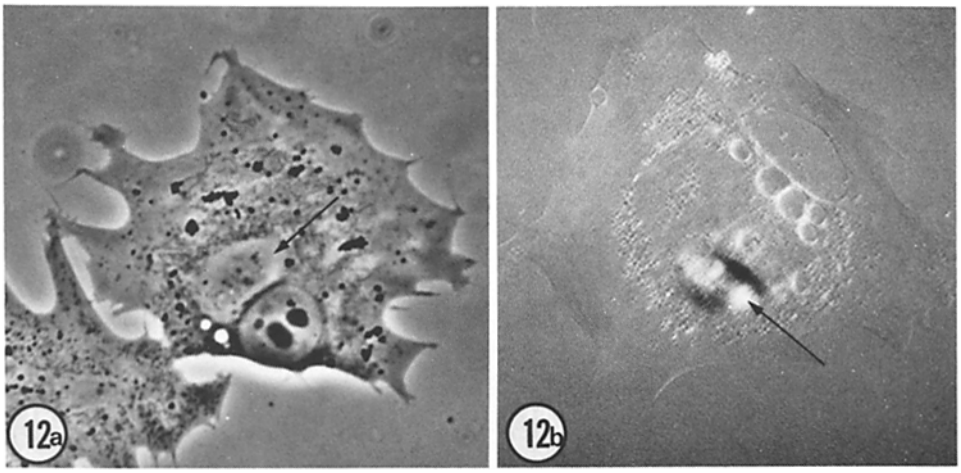

FIGURE 12 Formation of the juxtanuclear-birefringent region in cells treated with colchicine (10 μg/ml) for 3 h. The cells had attached and spread in normal medium for 3 h before the addition of colchicine. Fig. 12*a*: A cell viewed with phase-contrast optics that demonstrates the evident juxtanuclear clear region (arrow). × 560. Fig. 12*b*: A cell viewed with polarized-light optics showing the strong birefringence observed in the juxtanuclear region (arrow). × 560.

filaments. These observations suggest that these two fibrous components define channels along which organelles are dispersed.

Similar morphological relationships between microtubules and 10-nm filaments (neurofilaments) have been reported in nerve axons (30, 40, 41, 43, 44). We have also seen microtubule-10-nm filament associations in several other types of mammalian fibroblasts (unpublished observations). In other cell systems, microtubules alone have been implicated in organelle distribution (see for example, references 18, 20, 32, and 37).

Saltatory Movements

The translocation of organelles within the cytoplasm of BHK-21 cells is primarily saltatory in nature. Saltations occur at speeds ranging from 0.7 to 4.1 μm/s. These speeds are comparable to those measured in other cell types (9, 37). Rebhun (37) has suggested that both the maximum speed and the maximum path length of organelles vary inversely according to their size and the local viscosity of cytoplasm. These suggestions may ultimately help to explain in part the range of speed and SPL described in this study. In addition, the significant changes in speed, SPL, and direction of organelle movements which accompany spreading and shape formation in BHK-21 cells are closely related to the changes seen in the organization and localization of microtubules and 10-nm filaments. Intracellular movements described in other cell systems have also been related to the presence of cytoplasmic fibrillar components (see e.g., references 1–3, 5, 8, 14, 18, 28, 29, and 51). Therefore, the relationship between organelle movements and cytoplasmic fibers appears to be a general one.

Comparison of Intracellular Motility between Post-trypsinized Cells and Postmitotic Cells

Although the majority of observations have been made on BHK-21 cells during spreading after trypsinization and replating, similar changes in cell shape and in the complement of cytoplasmic fibers have been observed in daughter cells after mitosis (7, 13). BHK-21 cells gather together to divide, and after cytokinesis each daughter cell respreads on the substrate. During spreading, the changes in the pattern of intracellular birefringence and in the assembly and distribution of cytoplasmic fibers are similar to those that occur during the spreading process of a trypsinized cell (14, 13). In addition, we have found that there are changes in intracellular organelle distribution and saltatory movements in postmitotic cells which appear identical to the activities described in post-trypsinized cells (unpublished observations). Therefore, the information obtained in this study appears to be applicable to postmitotic cells, and may ultimately help to explain the redistribution of cytoplasmic organelles in spreading daughter cells after completion of cytokinesis.

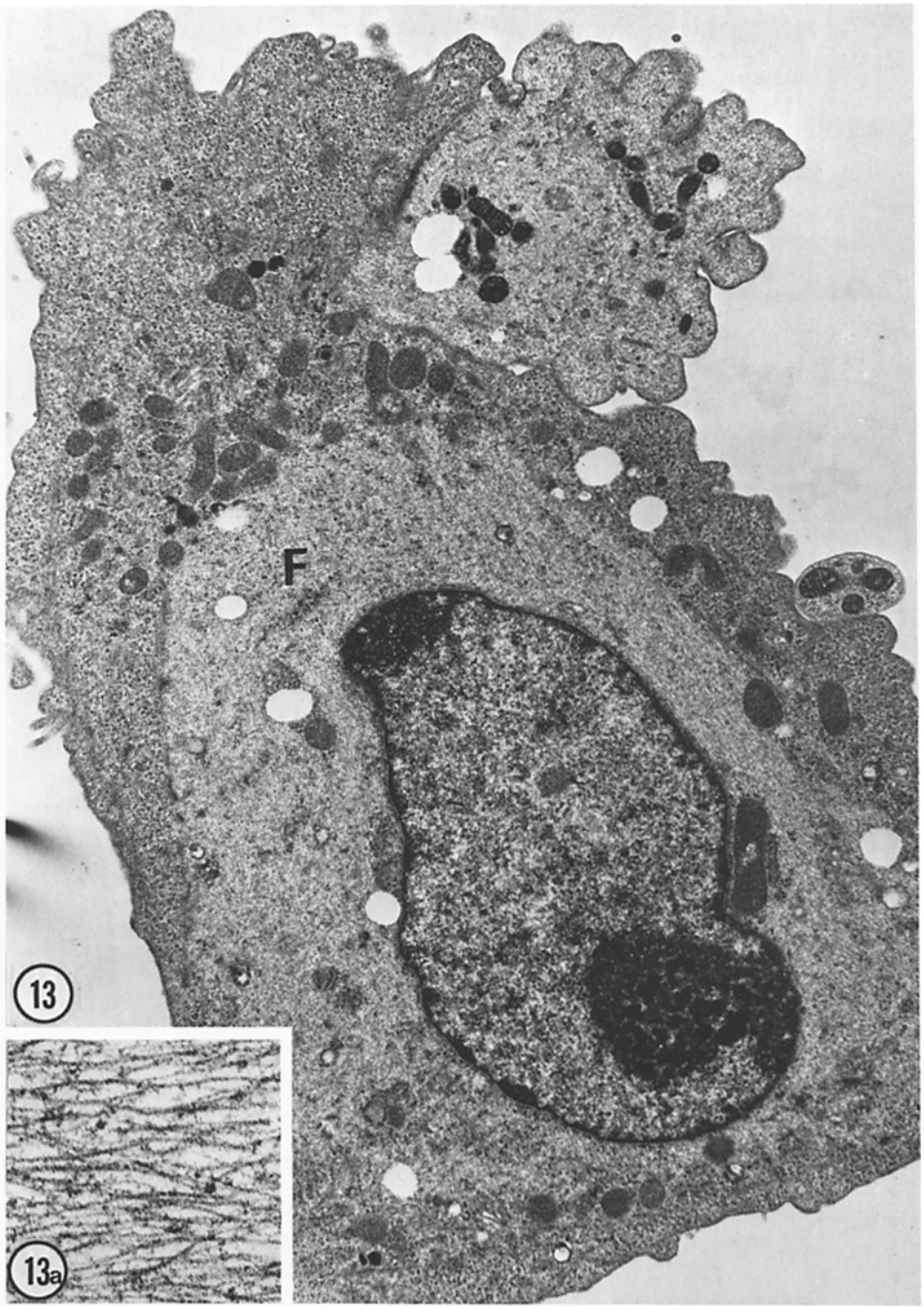

FIGURE 13 Electron micrograph of a colchicine-treated cell that demonstrates the juxtanuclear accumulation of 10-nm filaments (*F*). × 6,000. Fig. 13*a*: Higher magnification of 10-nm filament region. × 68,000.

Colchicine-Induced Cytoplasmic Streaming

Colchicine affects cell shape, locomotion, and pattern of intracellular birefringence in BHK-21 cells caused by the disappearance of microtubules and the formation of a juxtanuclear accumulation of 10-nm filaments (13, 14). In addition, the present study and those of Rebhun (35) and

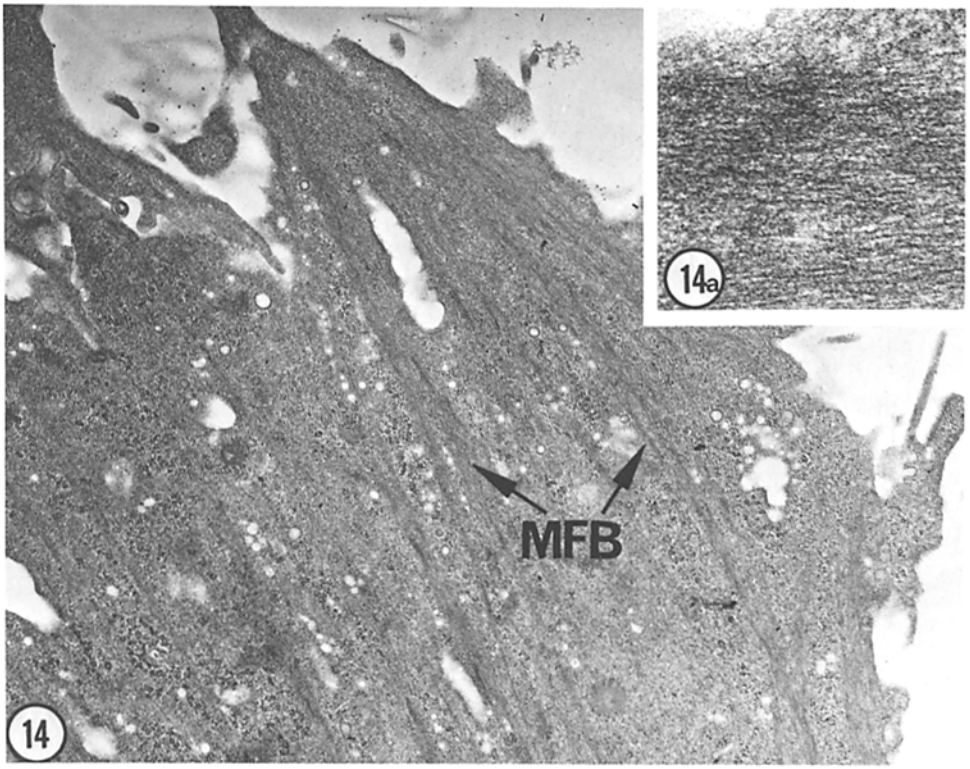

FIGURE 14 Electron micrograph of a cell treated with 10 μg/ml colchicine for 2 h. Note the abundance of microfilament bundles (*MFB*) adjacent to the adhesive surface of the cell. × 6,300. Fig. 14*a*: Higher magnification of microfilament bundle from a similar region. × 68,000.

Bhisey and Freed (4) demonstrate that the action of colchicine converts intracellular movements from a saltatory type to localized cytoplasmic streaming. As microtubule-10-nm filament associations are disrupted in colchicine-treated BHK-21 cells, organelles appear to move because of a bulk flow of cytoplasm which is reminiscent of the streaming cytoplasm seen in amoeboid organisms and acellular slime molds. These observations further indicate that a normal distribution of microtubule-10-nm filament complexes may oppose the bulk flow of cytoplasm by the formation of a rigid cytoskeletal network.

The results of this study also indicate that the streaming activity seen in colchicine-treated cells may be a direct reflection of the contractile nature of microfilament bundles. This possibility stems from the observation that actinlike microfilament bundles, which are capable of binding rabbit muscle HMM, are the only class of cytoplasmic fibers distributed within the streaming regions. Other evidence in support of the possible contractile nature of microfilament bundles stems from the immunofluorescence observations which indicate that the stress fibers that correspond to these bundles contain myosin, tropomyosin, and α-actinin (12, 15–17, 22–24, 50, 52).

SUMMARY

It must be emphasized that the exact nature of force-generation of intracellular organelle movements in BHK-21 cells, as well as other cell systems, remains unknown. The overall results from observations of normal and colchicine-treated cells indicate that microfilament bundles may generate the force for organelle movements and that microtubule-10-nm filament complexes may act as a cytoskeletal system involved in directing such movements. However, there is also the possibility that microtubules and 10-nm filaments are directly involved in motive force production. Possible cross bridges have been reported to exist between 10-nm filaments and microtubules in BHK-21 cells (14). It is therefore possible

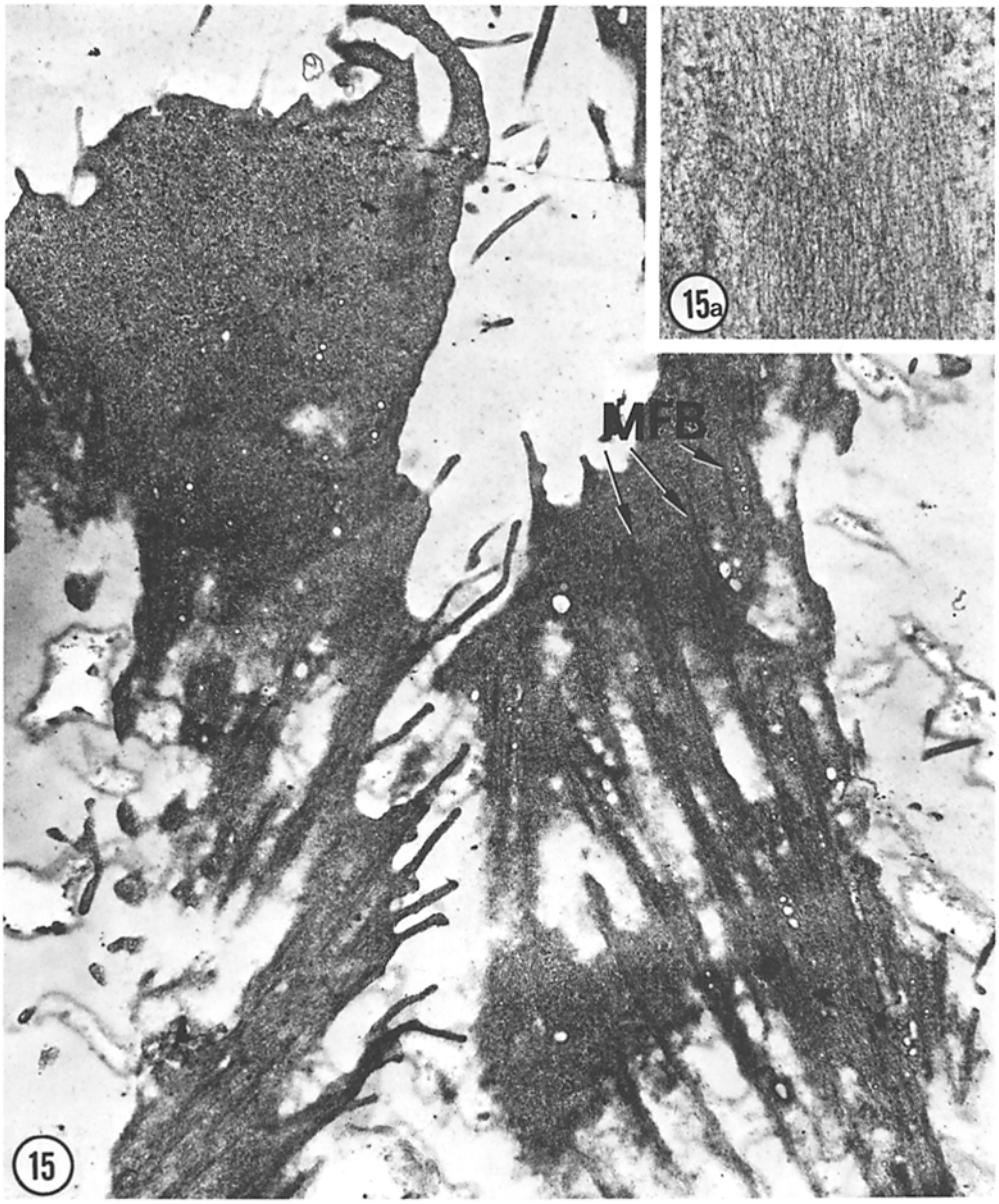

FIGURE 15 A section through the adhesive surface of a pseudopod that shows microfilament bundles (*MFB*). × 5,050. Fig. 15*a*: Higher magnification of microfilament bundles within a pseudopod. × 68,000.

that these two classes of fibers could move relative to each other and thus provide forces which are directly or indirectly involved in organelle movements. Obviously, a much more biochemical approach is needed to determine the nature of the relationships between 10-nm filaments and microtubules. The recent development of techniques for the isolation and biochemical characterization of 10-nm filaments from BHK-21 cells may pave the way for such investigations (45, 46).

We wish to thank Dr. C. M. Chang and Dr. J. S. Schloss for many thoughtful discussions. This work was performed in partial fulfillment for the PhD degree of E.

FIGURE 16 Electron micrograph of a thin section through a region of a pseudopod that is not adjacent to cell-substrate contact. Note ribosomes, pinocytotic vesicles, mitochondria (*M*), and lipid droplets (*L*). × 9,840.

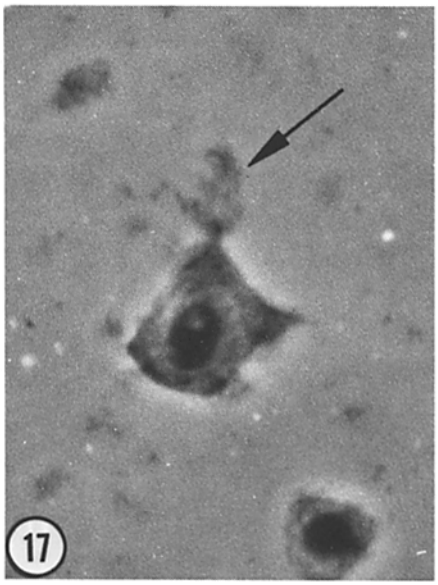

FIGURE 17 Glycerinated cell containing a pseudopod that has been flat embedded in Epon-812. The overall shape of the pseudopod (arrow) is retained. Phase contrast, × 480.

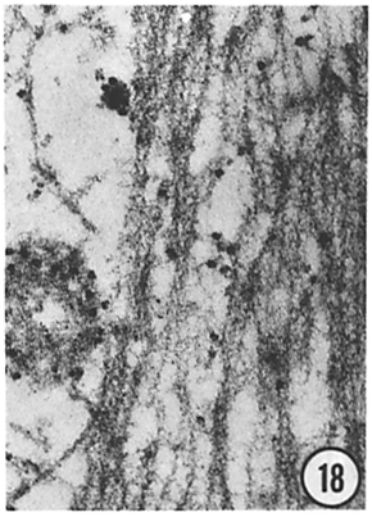

FIGURE 18 Electron micrograph of a thin section taken just beneath the plasma membrane of the substrate side of a pseudopod in a glycerinated-HMM. × 37,000.

Wang, and was supported by grants to R. D. Goldman from the National Cancer Institute (R01-CA-17210-03) and the National Science Foundation (BMS-73-01446 A01).

Received for publication 8 June 1977, and in revised form 25 July 1978.

REFERENCES

1. ALLEN, R. D., and R. R. COWDEN. 1962. Syneresis in amoeboid movement: its localization by interference microscopy and its significance. *J. Cell Biol.* **12**:185–189.
2. ALLERA, A., R. BECK, and K. E. WOHLFARTH-BOTTERMANN. 1971. Extensive fibrillar protoplasmic differentiations and their significance for protoplasmic streaming. VIII. Identification of the plasmafilaments in *Physarium polycephalum* as F-actin by *in situ* binding of heavy meromyosin. *Cytobiologie.* **4**:436–449.
3. ALLISON, A. C. 1973. Locomotion of tissue cells: The role of microfilaments and microtubules in cell movement, endocytosis, and exocytosis. *Ciba Found. Symp.* **14**:108–148.
4. BHISEY, A. N., and J. J. FREED. 1971. Amoeboid movement induced in cultured macrophage by colchicine or vinblastine. *Exp. Cell Res.* **64**:419–429.
5. BIKLE, D., L. G. TILNEY, and K. R. PORTER. 1966. Microtubules and pigment migration in the melanophores of *Fundulus heteroclitus*. *Protoplasma.* **61**:322–345.
6. CHANG, M. C., and R. D. GOLDMAN. 1973. The localization of actin-like fibers in cultured neuroblastoma cells as revealed by HMM binding. *J. Cell Biol.* **57**:867–874.
7. DICKERMAN, L. H. 1972. Cytoplasmic fibers and motile behavior of synchronized BHK-21 fibroblasts. *J. Cell Biol.* **55**(2, Pt. 2):60*a*. (Abstr.)
8. FINE, R. E., and D. BRAY. 1971. Actin in growing nerve cells. *Nat. New Biol.* **234**:115–120.
9. FREED, J. J., and M. M. LEBOWITZ. 1970. The association of a class of saltatory movements with microtubules in cultured cells. *J. Cell Biol.* **45**:334–354.
10. GOLDMAN, R. D. 1971. The role of three cytoplasmic fibers in BHK-21 cell motility. I. Microtubules and the effects of colchicine. *J. Cell Biol.* **51**:752–762.
11. GOLDMAN, R. D. 1972. The effects of cytochalasin B on the microfilaments of baby hamster kidney (BHK-21) cells. *J. Cell Biol.* **52**:246–254.
12. GOLDMAN, R. D. 1975. The use of heavy meromyosin binding as an ultrastructural cytochemical method for localization and determining the possible functions of actin-like microfilaments in non-muscle cells. *J. Histochem. Cytochem.* **23**(7):529–542.
13. GOLDMAN, R. D., G. BERG, A. BUSHNELL, C. CHANG, L. DICKERMAN, N. HOPKINS, M. L. MILLER, R. POLLACK, and E. WANG. 1973. Locomotion of tissue cells. Fibrillar systems in cell motility. *Ciba Found. Symp.* **14**:83–107.
14. GOLDMAN, R. D., and D. KNIPE. 1973. The functions of cytoplasmic fibers in non-muscle cell motility. *Cold Spring Harbor Symp. Quant. Biol.* **37**:523–533.
15. GOLDMAN, R. D., E. LAZARIDES, R. POLLACK, and K. WEBER. 1975. The distribution of actin in non-muscle cells: The use of actin antibody in the localization of actin with the microfilament bundles of mouse 3T3 cells. *Exp. Cell Res.* **90**:333–334.
16. GOLDMAN, R. D., J. A. SCHLOSS, and J. M. STARGER. 1976. Organizational changes of microfilaments during animal movement. *Cold Spring Harbor Conf. Cell Proliferation.* **3**:217–246.
17. GOLDMAN, R. D., M. J. YERMA, and J. SCHLOSS. 1976. Localization and organization of microfilaments and related proteins in normal and virus-transformed cells. *J. Supramol. Struct.* **5**:155–183.
18. HOLMES, K., and P. W. CHOPPIN. 1968. On the role of microtubules in movement and alignment of nuclei in virus-induced syncytia. *J. Cell Biol.* **51**:752–762.
19. JAHN, T. L., and E. C. BOVEE. 1969. Protoplasmic movements within cells. *Physiol. Rev.* **49**:793–861.
20. JUNQUEIRA, L. C., and K. R. PORTER. 1969. Mechanisms for pigment migration in melanophores and erythrophores. *J. Cell Biol.* **43**(2, Pt. 2):62*a*.
21. KOMNICK, H., W. STOCKEM, and K. R. WOHLFARTH-BOTTERMANN. Cell motility: Mechanisms in protoplasmic streaming and amoeboid movement. *Fortschr. Zool.* **21**:1–74.
22. LAZARIDES, E. 1975. Tropomyosin antibody: the specific localization of tropomyosin in non-muscle cells. *J. Cell Biol.* **65**:549–561.
23. LAZARIDES, E. 1976. Actin, α-actinin, and tropomyosin interaction in the structural organization of actin filaments in non-muscle cells. *J. Cell Biol.* **68**:202–219.
24. LAZARIDES, E., and K. WEBER. 1974. Actin antibody: the specific visualization of actin filaments in non-muscle cells. *Proc. Natl. Acad.*

Sci. U. S. A. **71**:2268–2272.

25. LOCKE, M., and N. KRISHNAN. 1971. Hot alcoholic phosphotungstic acid and uranyl acetate as routine stains for thick and thin sections. *J. Cell Biol.* **50**:550–557.
26. LUFT, J. H. 1961. Improvements in epoxy resin embedding method. *J. Biophys. Biochem. Cytol.* **9**:409–414.
27. MCINTOSH, J. R. 1974. Bridges between microtubules. *J. Cell Biol.* **61**:186–187.
28. MURPHY, D. B., and L. G. TILNEY. 1974. The role of microtubules in the movement of pigment granules in teleost melanophores. *J. Cell Biol.* **61**:757–779.
29. MURPHY, R. L., and M. W. DUBIN. 1975. The occurrence of actin-like filaments in association with migrating pigment granules in frog retinal pigment epithelium. *J. Cell Biol.* **64**:705–710.
30. PETERS, A., S. L. PALAY, and H. WEBSTER. 1970. The Fine Structure of the Nervous System. Harper and Row Publishers, Inc., New York. 198.
31. POLLARD, T. D., and R. R. WEIHING. 1974. Cytoplasmic actin and myosin and cell movement. *In* CRC Critical Reviews in Biochemistry. G. D. Fasman, editor. **2**:1–65. Chemical Rubber Co., Cleveland, Ohio.
32. PORTER, K. R. 1973. Locomotion of tissue cells. Microtubules in intracellular locomotion. *Ciba Found. Symp.* **14**:149–169.
33. REBHUN, L. I. 1959. Studies of early cleavage in the surf clam, *Spisula solidissima*, using methylene blue and toluidine blue as vital stains. *Biol. Bull.* (*Woods Hole*). **117**:518–545.
34. REBHUN, L. I. 1964. Saltatory particle movements in cells. *In* Primitive Motile Systems in Cell Biology. R. D. Allen and N. Kamiya, editors. Academic Press, New York. 503–525.
35. REBHUN, L. I. 1963. Induced amoeboid movement in eggs of surf clam *Spisula solidissima*. *Exp. Cell Res.* **29**:593–602.
36. REBHUN, L. I. 1967. Structural aspects of saltatory particle movement. *In* The Contractile Process. A. Stracher, editor. Little, Brown and Co., Boston. 223.
37. REBHUN, L. I. 1972. Polarized intracellular particle transport: Saltatory movements and cytoplasmic streaming. *Int. Rev. Cytol.* **32**:93–131.
38. REYNOLDS, R. 1963. The use of lead citrate at high pH as an electron opaque stain in electron microscopy. *J. Cell Biol.* **17**:208–212.
39. SCHLOSS, J. A., A. MILSTED, and R. D. GOLDMAN. 1977. Myosin subfragment binding for the localization of actin-like microfilaments in cultured cells. A light and electron microscope study. *J. Cell Biol.* **74**:794–815.
40. SCHMITT, F. O. 1968. The molecular biology of neuronal fibrous proteins. *Neurosci. Res. Program Bull.* **6**:119–144.
41. SCHMITT, F. O. 1968. Fibrous proteins—neuronal organelles. *Proc. Natl. Acad. Sci. U. S. A.* **60**:1092–1104.
42. SCHROEDER, T. E. 1972. The contractile ring. II. Determining its brief existence, volumetric changes, and vital role in cleaving *Arbacia* eggs. *J. Cell Biol.* **53**:419–434.
43. SHELANSKI, M. L., S. H. YEN, and V. M. LEE. 1976. Neurofilaments and glial filaments. *Cold Spring Harbor Conf. Cell Proliferation.* **3**:1007–1020.
44. SMITH, D. S., V. JALFORS, and B. F. CAMERON. 1975. Morphological evidence for the participation of microtubules in axonal transport. *Ann. N. Y. Acad. Sci.* **253**:472–506.
45. STARGER, J., W. BROWN, A. GOLDMAN, and R. D. GOLDMAN. 1978. Biochemical and immunological analysis of rapidly purified 10-nm filaments from baby hamster kidney (BHK-21) cells. *J. Cell Biol.* **78**:93–109.
46. STARGER, J., and R. D. GOLDMAN. 1977. Isolation and preliminary characterization of 10-nm filaments from baby hamster kidney (BHK-21) cells. *Proc. Natl. Acad. Sci. U. S. A.* **74**:2422–2426.
47. STOKER, M. G. P., and I. MACPHERSON. 1964. Syrian hamster fibroblast cell line BHK-21 and its derivatives. *Nature* (*Lond.*). **203**:1355–1356.
48. SZENT-GYORGI, A. G. 1953. Meromyosin, the subunits of myosin. *Arch. Biochem. Biophys.* **42**:305–320.
49. TAYLOR, E. W. 1965. Brownian and saltatory movements of cytoplasmic granules and the movement of anaphase chromosomes. Proc. of the 4th Intern. Cong. on Biorheology. Wiley-Interscience, New York. 503.
50. WEBER, K., and U. GROSCHEL-STEWART. 1974. Antibody to myosin: The specific visualization of myosin-containing filaments in non-muscle cells. *Proc. Natl. Acad. Sci. U. S. A.* **71**:4561–4564.
51. WOHLFARTH-BOTTERMANN, K. D. 1964. Differentiations of the ground cytoplasm and their significance for the generation of the motive force of ameboid movement. *In* Primitive Motile Systems in Cell Biology. R. A. Allen and N. Kamiya, editors. Academic Press, New York. 79–110.
52. YERNA, M. J., M. O. AKSOY, D. J. HARTSHORNE, and R. D. GOLDMAN. 1978. BHK-21 myosin: Isolation, biochemical characterization and intracellular localization. *J. Cell Science.* **31**:411–429.